

Effect of Sputtering Pressure on Al-doped ZnO Films by DC Magnetron Sputtering

SUN Ke-Wei, ZHOU Wan-Cheng, HUANG Shan-Shan, TANG Xiu-Feng

(State Key Laboratory of Solidification Processing, School of Materials Science and Engineering, Northwestern Polytechnical University, Xi'an 710072, China)

Abstract: Al-doped ZnO (AZO) films were deposited on the glass substrates by direct current magnetron sputtering using different sputtering pressures ranging from 0.2 Pa to 2.2 Pa. Microstructure, phase, electrical and optical properties of AZO films were characterized by X-ray diffraction (XRD), scanning electron microscope (SEM), four-point probe and UV-Vis spectrophotometer, respectively. The results revealed that the deposition rate decreased with the increasing sputtering pressure according to Keller-Simmons model; the crystalline phase of all films was hexagonal wurtzite and the preferred orientation changed with the sputtering pressure; the surface morphology greatly depended on the sputtering pressure and the film deposited at 1.4 Pa showed low resistivity ($8.4 \times 10^{-4} \Omega \cdot \text{cm}$), high average transmission and the highest Q , a criterion factor as the film figure of merit, which was the ratio between the normalized average transmission and the normalized resistivity.

Key words: Al-doped ZnO films; direct current magnetron sputtering; sputtering pressure; electro-optical property

Transparent conductive oxide (TCO) thin films have been widely used as transparent electrodes in opto-electronic devices such as solar cells^[1] and flat panel displays^[2] due to their characteristics of low resistivity, high visible transmittance and high infrared reflectance. The main transparent electrode material currently used in the opto-electronic industries is indium tin oxide (ITO) because of its excellent optical and electrical properties^[3-5]. However, Al-doped ZnO (AZO) films have attracted more attention in recent years over ITO films, due to their many advantages including low cost, non-toxicity, material abundance and high stability to H₂ plasma^[6-7].

AZO films have different conductivity, transparency and surface structure depending upon deposition methods. There are many deposition techniques such as DC or RF magnetron sputtering^[8-10], Sol-Gel process^[11] and pulsed laser deposition^[12]. However, the most frequently used deposition technique is DC magnetron sputtering which provides high deposition rate, perfect adhesion and large deposition area^[13]. Properties of DC sputtered AZO films are sensitive to sputtering parameters: total sputtering pressure, substrate temperature, sputtering power, target to substrate distance, oxygen content in sputtering gas and target quality.

Some investigations have been reported about effects of the sputtering pressure on AZO films by DC magnetron

sputtering. However, there is no systemic research on the microstructure of AZO films depending on the pressure, which is critical for their electro-optical properties. In this study, direct current magnetron sputtering was adopted to prepare AZO films using different sputtering pressures. Influences of sputtering pressure on crystalline phase, surface structure and electro-optical properties were discussed in detail.

1 Experimental

AZO films were deposited on the glass substrates at different sputtering pressures ranging from 0.2 Pa to 2.2 Pa by direct current magnetron sputtering using JPG450 sputtering system. A commercially available sintered ceramic ZnO:Al (2wt% Al₂O₃) target (99.99% purity) of 60 mm in diameter was employed. Before deposition, glass substrates were ultrasonically cleaned in acetone, distilled water and ethanol, successively. The target to substrate distance was 6.5 cm. The background pressure was 6.6×10^{-4} Pa and the substrate temperature was kept at 200°C in the sputtering. A DC power of 34 W was used for all samples and the sputtering time was 40 min.

The film thickness was examined using a surface profiler (Ambios, XP2). The crystalline phase was examined by X-ray powder diffraction analysis using a CuK α radi-

Received date: 2012-04-06; Modified date: 2012-05-28; Published online: 2012-07-10

Foundation item: National Natural Science Foundation of China (51072165)

Biography: SUN Ke-Wei(1979-), female, candidate of PhD. E-mail: sun_kewei@yeah.net

Corresponding author: ZHOU Wan-Cheng, professor. E-mail: wczhou@nwpu.edu.cn

tion (Philips χ^2 Pert diffractometer). The microstructure was observed with a scanning electron microscope (SEM) (JSM-6360, Japan). The electrical resistivity was obtained using standard four-point probe measurement. The optical properties were measured by UV-Vis spectrophotometer (Shimadzu uv3150, Japan).

2 Results and discussion

2.1 Deposition rate

The film thickness was examined using a surface profiler, and the thicknesses of films deposited at 0.2, 0.6, 1.0, 1.4, 1.8 and 2.2 Pa are 346, 298, 268, 129, 122 and 110 nm, respectively. The dependence of the deposition rate on sputtering pressure is shown in Fig. 1. As predicted by Keller and Simmons^[14], the deposition rate decreases with increasing argon pressure according to the Equation

$$R = R_0 \frac{(pd)_0}{Pd_{ST}} \left(1 - e^{-\frac{Pd_{ST}}{(pd)_0}}\right) \quad (1)$$

Where R_0 is the deposition rate pre-factor, P is the pressure inside the sputtering chamber, d_{ST} is the sample-target distance and $(pd)_0$ is the pressure-distance parameter describing the mean free path of sputtered atoms at a certain pressure. Its value can be determined by fitting the Equation (1) to the measured deposition rate^[15]. Here fitting parameters include a deposition rate pre-factor $R_0=9.98$ nm/min and $(pd)_0=55$ Pa·cm.

2.2 Crystalline phase

Figure 2 shows the XRD patterns of the AZO films deposited at sputtering pressures of 0.2, 0.6, 1.0, 1.4, 1.8 and 2.2 Pa, respectively. The crystalline phase of all films is hexagonal wurtzite.

The film deposited at 0.2 Pa shows a strong peak of (002) and a weaker peak of (103), which is in agreement with the reports^[16-18]. With increasing the sputtering pressure to 1.0, 1.4 Pa, the (101) and (100) peaks appear re-

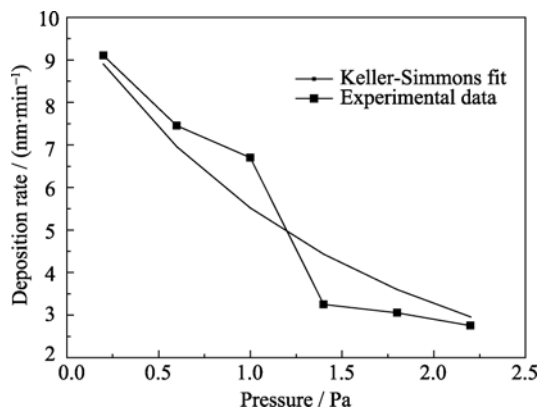


Fig. 1 Dependence of deposition rate on sputtering pressure. The solid curve is the fitting line according to Keller-Simmons model

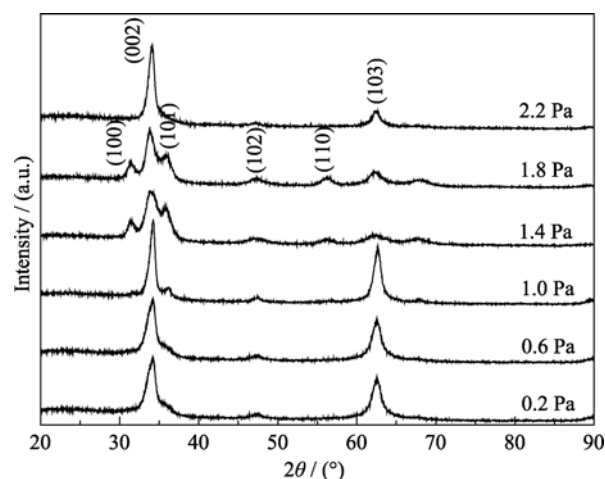


Fig. 2 XRD patterns of the AZO films deposited at different sputtering pressures

spectively. At the same time, the (103) peak becomes weaker. However, when the sputtering pressure is up to 2.2 Pa, the films have strong (002) peak and show obvious preferred orientation of (002).

In general, the textured film growth can be realized either by an evolution competition process of the statistically oriented grains or by a particle flux-determined selective growth process. In the former case, the so-called van der Drift mechanism, only grains with their fastest crystal growth direction parallel to the film growth direction can survive while other grains will be overgrown. In the latter case, grains with a certain special orientation will be allowed to grow by ion impact while the growth of other grains will be suppressed due to a selective ion etching or resputtering process^[19].

As to the film growth in this work, the van der Drift mechanism can be ruled out. The growth of (002), (101) and (100) faces are fast, and $v(002) > v(101) > v(100)$, according to Li^[20]. The fast growth is mainly due to the low surface energy. With the increasing sputtering pressure, the deposition rate of the film decreases, which is useful for horizontal migration of atoms. The atoms will migrate to these faces possessing low surface energy. So, the (101) and (100) peak appear respectively with the increasing sputtering pressure to 1.0, 1.4 Pa, and up to 2.2 Pa, the film shows obvious preferred orientation of (002).

2.3 Film microstructure

The scanning electron microscope images of AZO films have been taken to evaluate their surface morphology and microstructure. Figure 3 shows the surface micrographs of films as a function of the sputtering pressure. It is found that the sputtering pressure has a great influence on film surface structure. The film deposited at the sputtering pressure of 0.2 Pa shows surface features of densely packed fibrous grains (4 nm) and gains aggregate-

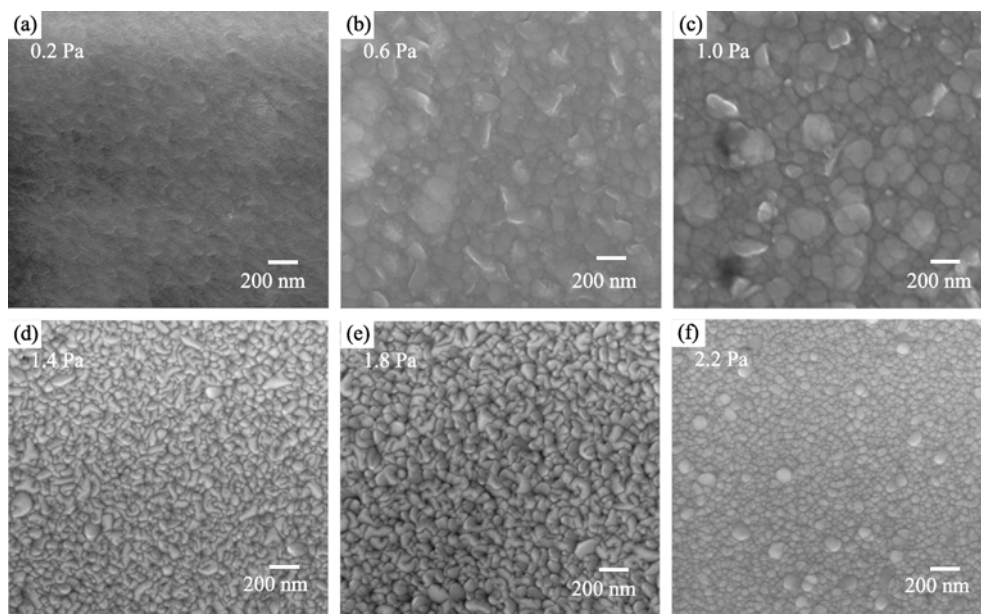


Fig. 3 SEM images of the AZO films deposited at different sputtering pressures

ing. The films deposited at 0.6 Pa and 1.0 Pa show surface features of mainly hexagonal and some other shapes and the particle size becomes larger. The films deposited at 1.4 Pa and 1.8 Pa show surface features of uniform particle shape and particle size. The film deposited at 2.2 Pa shows perfect hexagonal structure. The results from the surface micrographs of films are quite consistent with XRD analysis as shown in Fig. 2.

The deposition rate is high at 0.2 Pa and the atoms deposited on the substrate are prevented by new arriving atoms from further diffusing in the film. Meanwhile, new nuclei are continuously formed in the process of deposition, leading to small critical nucleation in the film. Therefore, the film deposited at 0.2 Pa shows surface features of densely packed fibrous grains. The deposition rate decreases with the increasing sputtering pressure, which is useful for horizontal migration of atoms. Further, the crystalline size becomes larger and so uniform columnar structure is formed in the film and the grain surface begins to form unique crystallographic morphology. At higher sputtering pressures, grains in the film surface form regular and close hexagonal arrangement, and meanwhile the crystallization is improved.

2.4 Electro-optical properties

Figure 4 shows the resistivity variation of films depending upon the sputtering pressure. The resistivity of the films decreases greatly with the increasing sputtering pressure ranging from 0.2 Pa to 1.0 Pa, and then increases lightly with the increasing sputtering pressure ranging from 1.4 Pa to 2.2 Pa. A minimum resistivity value of $8.4 \times 10^{-4} \Omega \cdot \text{cm}$ is seen at 1.4 Pa. This result is in agreement with Zhu's report^[21].

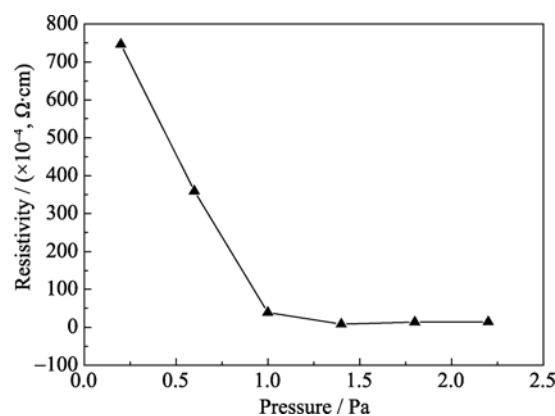


Fig. 4 Resistivity of the AZO films as a function of sputtering pressure

The resistivity of semiconductor materials is determined according to the Equation,

$$\rho = \frac{1}{\sigma} = \frac{1}{ne\mu} \quad (2)$$

Where, n is carrier concentration, μ is carrier mobility, and e is electronic unit. The mobility in the film is affected by scattering and the carrier concentration is mainly affected by the Al dopant. The greatly decreasing resistivity in the pressure range of 0.2 Pa to 1.0 Pa may be due to the increasing grain size (as shown in Fig. 3), which could decrease the grain boundary scattering and brings an increase of carrier mobility. At meantime, the decreasing deposition rate with the increasing sputtering pressure is useful for horizontal migration of atoms and more Al substitution, which brings an increase of carrier concentration.

The lightly increasing resistivity with the increasing sputtering pressure over the range of 1.4 Pa to 2.2 Pa may

be due to the small thickness of the films. The thickness of the transparent conductive film has a significant impact on the electrical properties^[22]. For the thicker films, the resistivity has no relationship with the thickness. However, the resistivity will increase with the decrease of the thickness, when the film is very thin.

The optical transmission spectra for visible and near-IR spectra of films are shown in Fig. 5. All investigated films show more than 80% transmission between 400 and 800 nm and more than 60% transmission over range of near-infrared wave.

A criterion parameter Q , which characterizes the electro-optical properties of films, was defined as the ratio of normalized average transmission to normalized resistivity:

$$Q = \frac{\text{Norm.}(T_{\text{ave}})}{\text{Norm.}(\text{resistivity})} \quad (3)$$

In this study, the average transmission and the resistivity of films have been normalized to 90% and $8 \times 10^{-4} \Omega \cdot \text{cm}$, respectively. The variation of Q with the sputtering pressure is shown in Fig. 6. It can be seen that the maximum value of Q obtained at 1.4 Pa is 0.9, which is mainly due to the minimum resistivity.

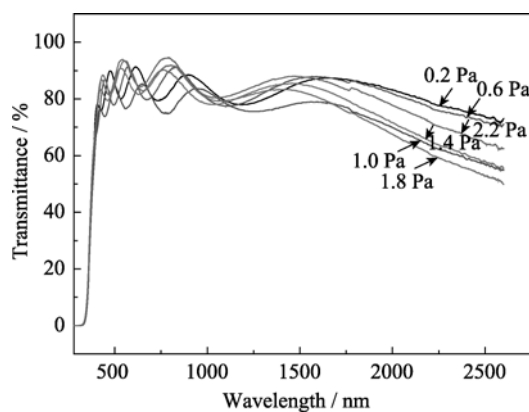


Fig. 5 Transmittance spectra of the AZO films deposited at different sputtering pressures

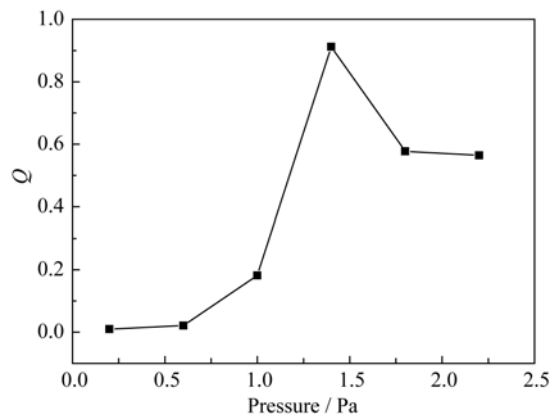


Fig. 6 Variation of Q with the sputtering pressure

3 Conclusion

1) The deposition rate decreases with the increasing sputtering pressure according to Keller-Simmons model.

2) With the increasing sputtering pressure, the film show the strong peaks of (002) and (103) firstly, and then the (101) and (100) peaks appear; finally, the film has the only strong (002) peak. These results appear because (002), (101) and (100) planes possess low surface energy.

3) The film surface structure is greatly depended on the sputtering pressure, which is consistent with the XRD result.

4) The film deposited at 1.4 Pa shows the lowest resistivity, high transparency and the highest Q value, mainly due to the uniform particle shape and particle size. The decrease of grain boundary scattering will bring on the weaker scattering process of carriers and photons in the AZO films.

References:

- [1] Kobayashi H, Ishida T, Nakato Y, *et al.* Mechanism of carrier transport in highly efficient solar cells having indium tin oxide/Si junctions. *J. Appl. Phys.*, 1991, **69**(3): 1736–1743.
- [2] Oh B Y, Jeong M C, Moon T H, *et al.* Transparent conductive Al-doped ZnO films for liquid crystal displays. *J. Appl. Phys.*, 2006, **99**(12): 124505–124508.
- [3] Kim H, Horwitz J S, Kushto G P, *et al.* Indium tin oxide thin films grown on flexible plastic substrates by pulsed-laser deposition for organic light-emitting diodes. *Appl. Phys. Lett.*, 2001, **79**(3): 284–286.
- [4] Pan Rongjun, Pan Shenghui, Zhou Juying, *et al.* Surface-modification of indium tin oxide nanoparticles with titanium dioxide by a nonaqueous process and its photocatalytic properties. *Appl. Surf. Sci.*, 2009, **255**(6): 3642–3647.
- [5] Fu En-Gang, Zhuang Da-Ming, Zhang Gong, *et al.* Substrate temperature dependence of the properties of ZAO thin films deposited by magnetron sputtering. *Appl. Surf. Sci.*, 2003, **217**(1-4): 88–94.
- [6] Nunes P, Fortunato E, Martins R. Influence of the post-treatment on the properties of ZnO thin films. *Thin Solid Films*, 2001, **383**(1/2): 277–280.
- [7] Natsume Y, Sakata H. Electrical and optical properties of zinc oxide films post-annealed in H_2 after fabrication by Sol-Gel process. *Mater. Chem. Phys.*, 2002, **78**(1): 170–176.

- [8] Lee Jae-Hyeong, Song Jun-Tae. Dependence of the electrical and optical properties on the bias voltage for ZnO:Al films deposited by r.f. magnetron sputtering. *Thin Solid Films*, 2008, **516(7)**: 1377–1381.
- [9] Suche M, Christoulakis S, Katsarakis N, *et al.* Comparative study of zinc oxide and aluminum doped zinc oxide transparent thin films grown by direct current magnetron sputtering. *Thin Solid Films*, 2007, **515(16)**: 6562–6566.
- [10] Oda Jun-ichi, Nomoto Jun-ichi, Miyata Toshihiro, *et al.* Improvements of spatial resistivity distribution in transparent conducting Al-doped ZnO thin films deposited by DC magnetron sputtering. *Thin Solid Films*, 2010, **518(11)**: 2984–2987.
- [11] Zhu Dongmei, Li Kun, Luo Fa, *et al.* Preparation and infrared emissivity of ZnO: Al (AZO) thin films. *Appl. Surf. Sci.*, 2009, **255(12)**: 6145–6148.
- [12] Mass J, Bhattacharya P, Katiyar R S. Effect of high substrate temperature on Al-doped ZnO thin films grown by pulsed laser deposition. *Mater. Sci. Eng. B*, 2003, **103(1)**: 9–15.
- [13] Betz U, Olsson M K, Marthy J, *et al.* Thin films engineering of indium tin oxide: large area flat panel displays application. *Surf. Coat. Technol.*, 2006, **200(20/21)**: 5751–5759.
- [14] Keller J H, Simmons R G. Sputtering process model of deposition rate. *IBM J. Res. Develop.*, 1979, **23(1)**: 24–32.
- [15] Drüsedau T P, Löhmann M, Klabunde F, *et al.* Investigations on energy fluxes in magnetron sputter-deposition: implications for texturing and nanoporosity of metals. *Surf. Coat. Technol.*, 2000, **133-134**: 126–130.
- [16] Lin Wei, Ma Ruixin, Shao Wei, *et al.* Structural, electrical and optical properties of Gd doped and undoped ZnO:Al (ZAO) thin films prepared by RF magnetron sputtering. *Appl. Surf. Sci.*, 2007, **253(11)**: 5179–5183.
- [17] Li Tengfei, Qiu Hong, Wu Ping, *et al.* Characteristics of Ni-doped ZnO:Al films grown on glass by direct current magnetron co-sputtering. *Thin Solid Films*, 2007, **515(7/8)**: 3905–3909.
- [18] Suche M, Christoulakis S, Katsarakis N, *et al.* Comparative study of zinc oxide and aluminum doped zinc oxide transparent thin films grown by direct current magnetron sputtering. *Thin Solid Films*, 2007, **515(16)**: 6562–6566.
- [19] Jiang X, Jia C L, Szyszka B. Manufacture of specific structure of aluminum-doped zinc oxide films by patterning the substrate surface. *Appl. Phys. Lett.*, **80(17)**: 2090–3092.
- [20] LI W J, SHI E W, ZHONG W Z, *et al.* Growth mechanism and growth habit of oxide crystals. *Journal of crystal growth*, 1999, **203(1/2)**: 186–196.
- [21] Zhu H, Hüpkes J, Bunte E, *et al.* Influence of working pressure on ZnO:Al films from tube targets for silicon thin film solar cells. *Thin Solid Films*, 2010, **518(17)**: 4997–5002.
- [22] JIANG Xin, SUN Chao, HONG Rui-jiang, *et al.* Transparent Conductive Oxide Films. Beijing: Higher Education Press, 2008: 205.

溅射气压对直流磁控溅射 ZnO:Al 薄膜的影响

孙可为, 周万城, 黄珊珊, 唐秀凤

(西北工业大学 材料科学与工程学院, 凝固技术国家重点实验室, 西安 710072)

摘要: 采用直流磁控溅射法在玻璃基片上沉积 ZnO:Al(AZO)薄膜, 溅射气压为 0.2~2.2 Pa。通过 X 射线衍射(XRD)、扫描电子显微镜(SEM)、四探针和紫外-可见分光光度计对 AZO 薄膜的相结构、微观形貌和电光学性质进行了表征。结果表明: 薄膜的沉积速率随着溅射气压的增大而减小, 变化曲线符合 Keller-Simmons 模型; 薄膜均为六角纤锌矿结构, 但择优取向随着溅射气压发生改变; 溅射气压对薄膜的表面形貌有显著影响; 当溅射气压为 1.4 Pa 时, 薄膜有最低的电阻率($8.4 \times 10^{-4} \Omega \cdot \text{cm}$), 高的透过率和最高的品质因子 Q 。

关键词: ZnO:Al 薄膜; 直流磁控溅射; 溅射气压; 光电性质

中图分类号: TB34

文献标识码: A